Quick image display (QUID) model for rapid real-time target imagery and spectral signatures

Robert L. Sundberg[a], John Gruninger[a], Mark Nosek[b], Jeff Burks[c], and Ean Fontaine[c]

[a]Spectral Sciences, Inc., 99 South Bedford Street, Burlington, MA 01803
[b]Air Force Wright Lab, WPAFB, Dayton, OH 45433
[c]Tricor Systems, Inc., Dayton, OH 45432

ABSTRACT

The Quick Image Display (QUID) model accurately computes and displays radiance images at animation rates while the target undergoes unrestricted flight or motion. Animation rates are obtained without sacrificing radiometric accuracy by using three important innovations. First, QUID has been implemented using the OpenGL graphics library which utilizes available graphics hardware to perform the computationally intensive hidden surface calculations. Second, the thermal emission and reflectance calculations are factorized into angular and wavelength dependent terms for computational efficiency. Third, QUID uses OpenGL supported texture mapping to simulate pseudo curved surface reflectance. The size of the glint texture is controlled by paint/surface properties and the surface normals at the facet's vertices. QUID generates IR radiance maps, in-band and spectral signatures for high level of detail targets with thousands of facets. Model features are illustrated with radiance and radiance contrast images of aircraft.

Keywords: image, animation, reflectance, BRDF, emission, infrared, signature, virtual reality

1. INTRODUCTION

Rapid IR scene generation without restrictions on target location, target motion or observer motion is necessary for flight simulators and hardware in the loop seeker testing. It is a major challenge to develop the software capability to support this unrestricted motion without severely degrading image content or sacrificing radiometric accuracy. Spectral Sciences Inc., has developed the Quick Image Display (QUID) model to provide the capability of real-time target signature calculations.[1] QUID is designed around the OpenGL[2] graphics library and its use of high-speed, high-resolution, color-graphics workstation hardware to perform the more time-consuming aspects of the calculations, such as hidden surface calculations. In addition to utilizing the hardware of a workstation to perform the 3-D graphics computations it is also necessary to reformulate signature calculations so that a large fraction of the computation can be performed prior to display. We have developed a unique approach to the emissivity and reflectivity calculation which simultaneously satisfies energy conservation and is rapid enough to be used in a real-time application.

Our approach to emissivity and reflectance calculations allows the computation of the wavelength or bandpass quantities separately from the angular portions. This separation provides the basis for the fast accurate radiance calculations needed for real-time scene generation. The precomputation of bandpass quantities utilizes a factorization of the directional emittance and a partial factorization of the bidirectional reflectance into functions of wavelength and functions of target, observer and light source orientations. The approach makes explicit use of the mathematical structure of validated physical models. Computational speed is obtained not by approximations but by reorganizing the calculations to fully utilize graphics hardware.

QUID generates IR radiance maps, in-band and spectral signatures at animation rates. The current model is restricted to target emissions and solar reflections, but the detailed approach to include other signature components has been developed and work is in progress to add these additional signature components. A glint model is also being developed for QUID which utilizes the texture mapping features in OpenGL to produce rapid and accurate pseudo curved surface glints. The intensity and size characteristics of the glint are controlled by the paint/surface properties of the modeled facet and the facet's degree of surface curvature.

QUID offers several advantages over traditional techniques for target insertion applications, including the ability to determine the effects of atmospherics on the spatial degradation of individual signature components. Traditional approaches rely on precomputed target images which are "stitched" into background scenes. This is a tedious process when pixel resolutions between background and targets do not match; considerable averaging and smoothing are then required to complete the insertion and remove halos from edge pixels of the overlayed target. A second drawback with the "stitching" approach is that differing aspects must be created in advance, that is aspect angle variations along the flight path must be predetermined. Another drawback of "stitching" is that changes in the spatial distribution of the observed target radiance induced by changes in atmospheric path are ignored. Precomputed target images can only be scaled to account for changes in atmospheric transmittance. While total integrated signatures scale, individual components do not scale. Thus the individual contributions of emission, diffuse and specular solar reflectance, earthshine and skyshine, will contribute with different weights to the spatial target radiance distributions for each atmospheric path. Using the workstations' capabilities and our factorization approach to the emissivity and reflectance calculations permits inclusion of the changes in the spatial radiance distribution among the various signature components.

2. THE QUID MODEL

The fast target rendering capabilities of QUID are due to three main innovations. First, the workstation's hardware is used to perform the computationally intensive hidden surface calculations by using a depth buffer approach provided through an industry wide standard graphics interface called OpenGL. Second, the factorization of the directional emissivity and the bi-directional reflectance distribution function (BRDF) into angular and wavelength-dependent terms allows for precomputation of wavelength-dependent terms which do not change with target-observer angles. Third, texture mapping is used to provide a rapid simulation of curved surface glints. These innovations are discussed below.

2.1 OpenGL 3-D graphics rendering interface

OpenGL is a network transparent 3-D graphics rendering interface. Applications, like QUID, can generate high-quality pictures from user-defined graphical objects through low-level system commands. The OpenGL commands used by QUID are supported on all OpenGL systems either through low-level software commands or hardware accelerated configurations. This allows QUID to run on platforms ranging from multi-processor graphic super computers, from Silicon Graphics Inc. (SGI) and others, to PCs running Microsoft's Windows NT.

QUID uses the OpenGL to render the visible target surfaces doing the hidden surface calculations in the graphics hardware. OpenGL also supports lighting models, such as a lambertian diffuse lighting model and directional, or spot light models. Although these models are only qualitative they rely on the same source-observer angles used in the more sophisticated QUID lighting models. We are currently investigating the OpenGL lighting models with the hope of performing more of the observer-source angular calculations with the hardware accelerated OpenGL lighting models.

2.2 Factorized BRDF

The IR signature of a target is composed of five basic signature components including:

- target surface emissions,
- scattered solar radiation,
- scattered earthshine,
- scattered skyshine, and
- exhaust plume emission from hot molecular or particular species.

These basic signature components are illustrated in Figure 1. The QUID model factors each of these terms into their wavelength and angular dependent terms. Factorization allows QUID to precompute the wavelength dependent terms and obtain real-time display of the target IR image as the observer-target-source geometry changes.

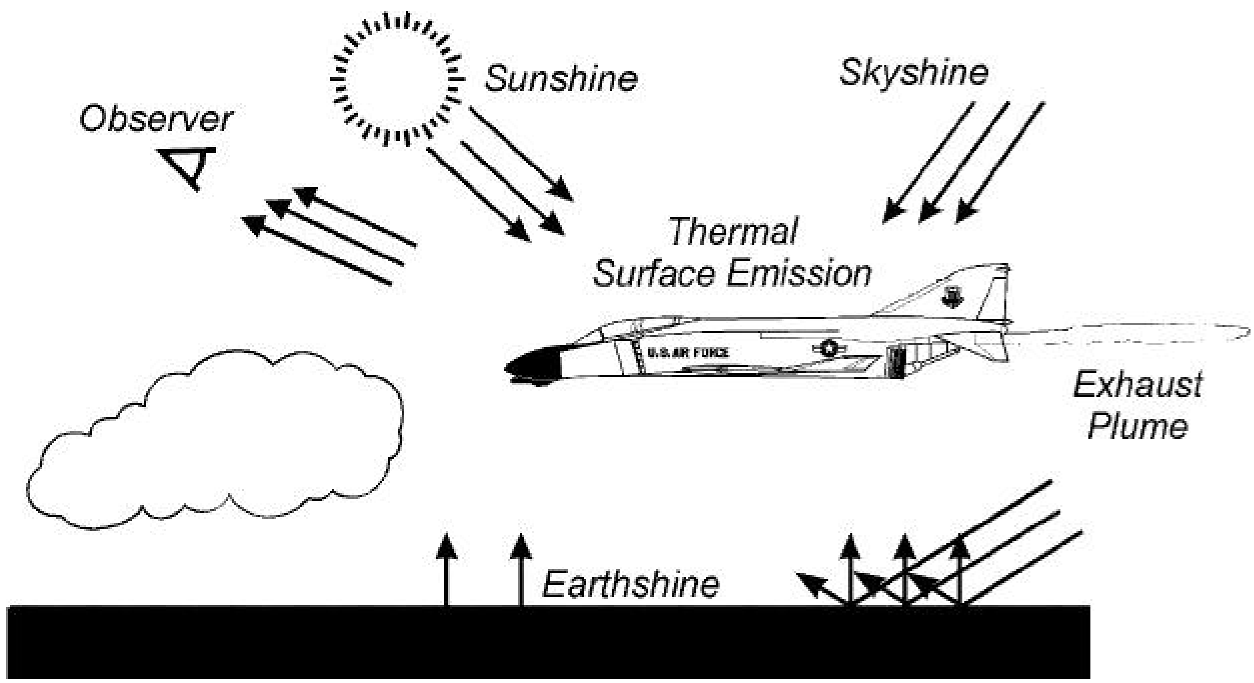

Figure 1. Schematic of an aircraft showing its IR signature components

The scattering of solar radiation, earthshine and skyshine depends on the bidirectional reflectance distribution function (BRDF), which completely defines the optical properties of opaque surfaces. The BRDF is defined as the surface reflectance for a given wavelength (ë), angles of incidence (è$_i$,ö$_i$) and angles of reflectance (è$_r$,ö$_r$). The angles are measured from the surface normal, **n̂,** to the observer and source vector, ô and ×, respectively. When a surface shows no preferential direction, or striae, the number of angles required to define the BRDF is reduced to three.

The BRDF can also be written in terms of the glint angle, á, and the scattering angle, ÷$_S$, see Figure 2. The glint vector is given by

$$\hat{g} = (\hat{\imath} + \hat{s}) / \sqrt{2(1+\hat{\imath}\bullet\hat{s})} \quad . \tag{1}$$

The glint angle, á, is defined as the angle between and the surface normal. $\hat{g}$ It is given by

$$cos\, a = \hat{g}\bullet\hat{n} \quad , \tag{2}$$

where n̂ is the direction of the surface normal. Note that á=0 corresponds to maximum specular reflection.

The BRDF, f$_r$(ë;á,÷$_S$) can be written as

$$f_r(\,l;a,c_S) = \sum_k r_k(\,l\,)\; F_k(a,c_S) \quad , \tag{3}$$

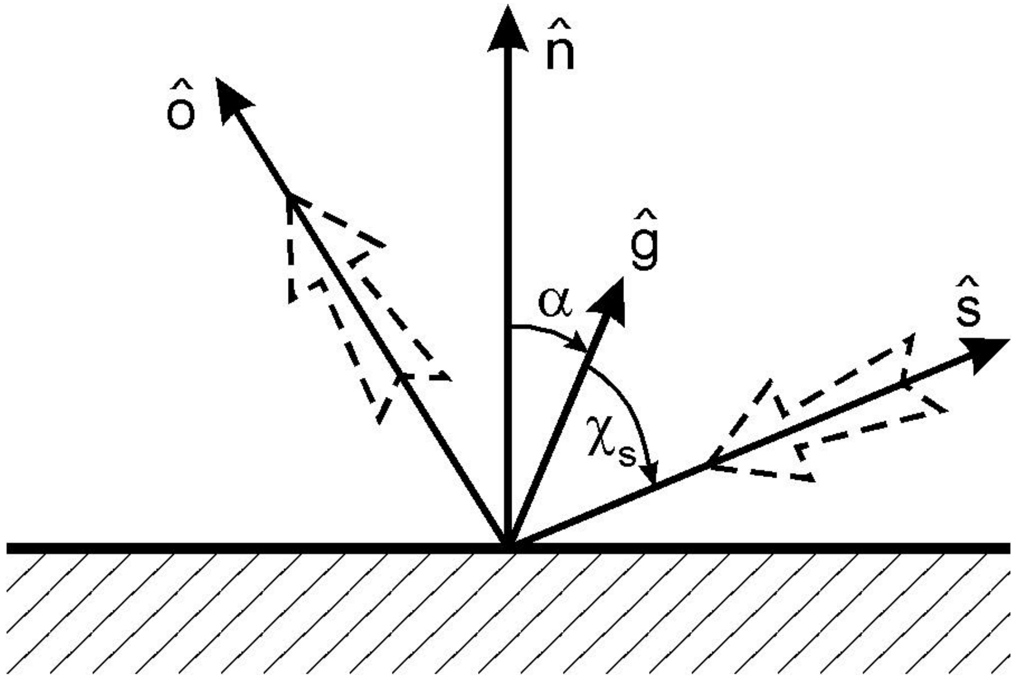

Figure 2. Angles for scattering by a surface element.

where the BRDF is represented as a sum of terms which are factored into wavelength, ñ$_k$(ë), and angular, F$_k$(á,÷$_S$), components. This representation of the BRDF is quite general and includes standard models such as the Sandford-Robertson[3] approach. During a QUID calculation the ñ$_k$(ë) terms are precomputed for a grid of observer-target ranges and a given bandpass. These terms include all of the atmospheric transmission effects that vary with range, but not with target orientation. The angular components in Equation 3 are then calculated each time the target-observer geometry changes.

2.3 Factorized directional emissivity

Another example of the factorization technique used in QUID is provided by examining the directional emissivity. The directional emissivity can be obtained from the measured total reflectance. It has been known for some time[3] that the directional emissivity can be taken as a product of a wavelength dependent function, the spectral emissivity, å$_ë$, and the angular falloff function, g(è$_O$) . Where è$_O$ is the angle between the observer and the surface normal.

$$e(l, q_O) = e_l \; g(q_O) \tag{4}$$

The evaluation of the contribution to the spectral apparent radiance of a target from thermal emission is found by the simple formula

$$L_l = \sum_i^N e_l \; g(q_i) \; B(l, T_i) \; t(l) \; a_i(q_i) \quad , \tag{5}$$

where B(ë,T_i) is the black body function for the ith surface, a_i(è$_i$) is its projected area and ô(ë) is the atmospheric transmittance and the sum is over all target facets. The equivalent in band apparent radiance requires an integration of $L_{ë}$ over the desired bandpass.

For high level of detail targets there may be thousands of facets and the revaluation of Equation 5 for each change in angle between observer and surface normal precludes its direct use for real time computation. Examination of Equation 5 reveals that the only angular dependence is found in g(è$_i$) a_i(è$_i$). This function is typically the only function that is strictly facet dependent since several facets may have the same temperature and hence the same black body function. The sum over facets can be replaced by a typically much shorter sum over unique temperature surfaces. Thus the apparent spectral radiance can be expressed as

$$L_l = \sum_{k}^{Temps} G_k \ A_k \{ e_l B(l ,T_k) t(l) \} \quad , \tag{6}$$

where $Ã_k$ is the area weighted average angular falloff function for the surface at temperature T_k

$$G_k = \sum_{i \in k} g(q_i) \ \frac{a(q_i)}{A_k} \tag{7}$$

and

$$A_k = \sum_{i \in k} a_i \tag{8}$$

is the total projected area of the surface at temperature T_k.

The quantities in brackets, $å_{ë}$B(ë,T_k)ô(ë), can be precomputed for each unique temperature surface over a grid of atmospheric paths. The average angular falloff functions and the total projected areas can be evaluated in real time by the workstation. It is the combined use of Equations 6 and 7 which allows the real time evaluation of target inband and spectral signatures in the QUID model. It should be emphasized that Equations 6 and 7 are not approximations to Equation 5, but rather a rearrangement into a more efficient form for computation.

2.4 Texture mapping technique for pseudo curved surface glints

It is important to include the effects of curvature for simulations which are dominated by solar (or other point sources) reflections. Curvature, or pseudo curvature is incorporated into QUID by means of a Phong Shading[4] (PS) algorithm. PS is a technique for inferring the curvature of a ensemble of flat facets from the normal unit vectors of their shared vertices. The normal for any point within a facet is computed by interpolating from the facet's set of vertex normals. Figure 3 shows a simple flat triangular facet with its vertices normals and interpolated interior normals. Once the normals for interior points are known the reflectance at each point can be accurately determined. This technique is used extensively in the CAD/CAM community to render images and is exact for the surfaces of ellipsoids. PS is normally applied on a pixel-by-pixel basis for a given scene, or facet. Application of pixel based PS techniques would be too computationally intensive for real-time applications.

A more rapid PS technique was suggested by Segal et al.[5] where the PS glint intensity map is precomputed for a given set of paint/surface BRDF properties and stored as a texture. The glint texture is mapped onto the flat facets by computing the reflectance vector at each of the facet's vertices and using these vectors to determine the texture coordinates for each vertex. This technique has several advantages:

- the same glint texture can be stretch or compressed to represent many degrees of curvature,
- OpenGL supports texture mapping which is often supported in the graphics hardware,
- multiple level-of-detail (LOD) textures can be stored and used as a function of apparent facet size, and
- textures can be precomputed for given paint BRDF's.

Figure 4A and 4B show sample glints for two surfaces. The surface normals at the vertices are also shown. Surface 4A has a high degree of pseudo curvature leading to a small circular glint. While surface 4B has no curvature leading to a flat facet glint. Both of these glints were produced using the same glint texture.

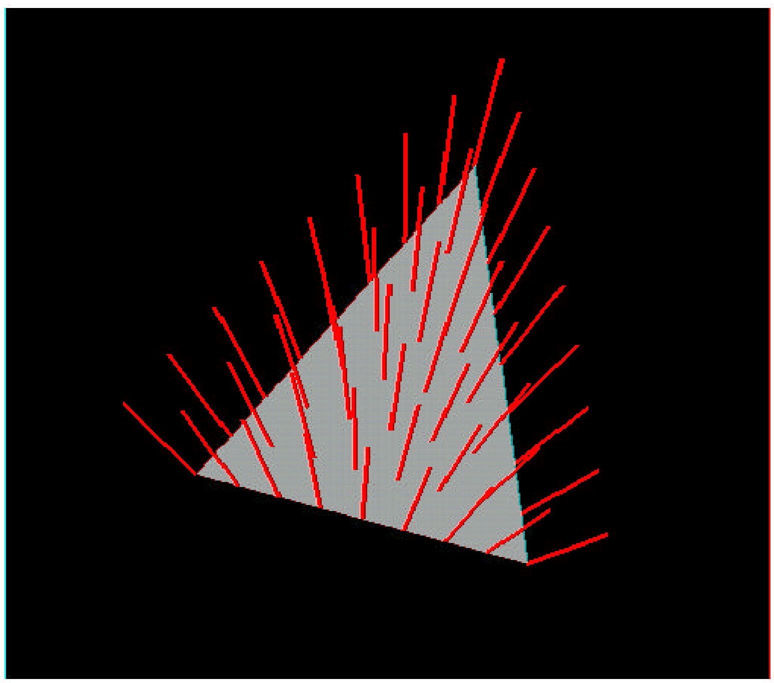

Figure 3. Facet vertices normals and interpolated interior normals.

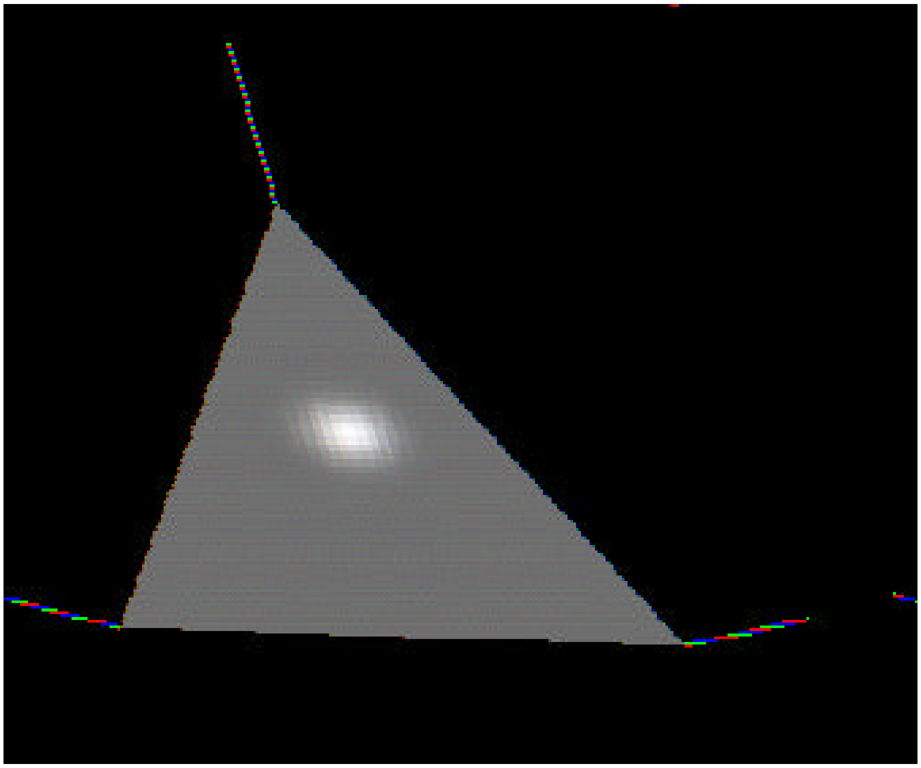

Figure 4 (A). Image of a solar glint using texture mapped Phong Shading algorthm for pseudo curved surface. Normals at vertices are also shown.

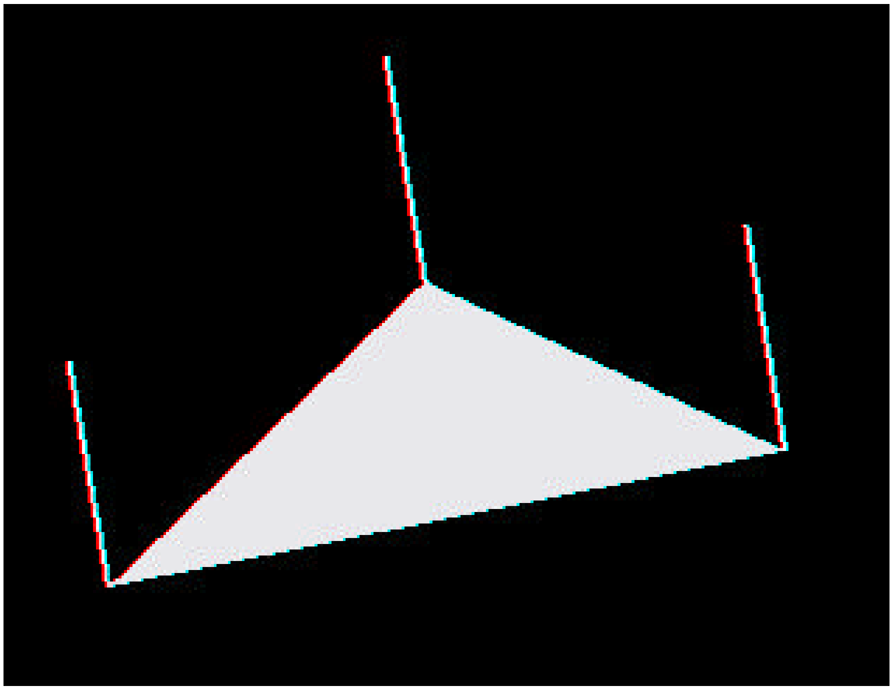

Figure 4 (B). Image of solar glint using texture mapped Phong Shading algorithm for a flat surface. The same texture map was used in both Figure 4(A) and (B). Normals at the vertices are also shown..

3. SAMPLE IMAGES

In this section we show a few sample images which illustrate the lighting and emission models found in QUID. Figure 5A shows a thermal emission radiance image for an aircraft at a near-broadside orientation. Figures 5B and 5C show the spatially integrated spectral radiance components for the image and the inband radiance contrast as a function of range for the aircraft orientation shown in Figure 5A. Spectral radiance and inband contrast radiance are available in QUID for a particular target orientation by simply clicking on a mouse-button.

Figure 6 shows a series of images for an aircraft as the observer aspect angle varies from just off nose-on to broad-side. These images include thermal emission and flat surface direct solar scattering. Notice that the solar glints off of the aircraft are the brightest radiance sources in the image. The images shown in Figure 6 also contain a simple model for aircraft plumes. The model is based on SIRRM[6] calculations for a predetermined spectral bandpass and plume facets generated from SIRRM axial and radial stations.

4. SUMMARY

The QUID model accurately displays radiance images at animation rates while the target undergoes unrestricted flight or motion. Animation rates are obtained without sacrificing radiometric accuracy by using three important innovations. First, QUID utilizes the graphics hardware on a variety of workstation platforms to perform the computationally intensive hidden surface calculations. Second, the thermal emission and reflectance calculations are factorized into angular and wavelength dependent terms. This allows the wavelength dependent terms to be precomputed before image display. Third, a fast texture mapped Phong Shading algorithm is under development for pseudo curved surface solar reflections. QUID generates IR radiance maps, in-band and spectral signatures for high level of detail targets with thousands of facets. Current upgrades to QUID include the addition of structured scene backgrounds and dynamic radiometrically accurate counter measures.

REFERENCES

1. J. H. Gruninger and A. Berk, "Quick Image Display Model: Final Report," Spectral Sciences, Inc. Rpt. No. SSI-TR-186 (March 1991).

2. J. Neider, T. Davis, M. Woo, and OpenGL Architecture Review Board, *OpenGL Programming Guide*, Addison-Wesley, Reading, MA (1993).

3. B. P. Sandford and D. C. Robertson, "Infrared Reflectance Properties of Aircraft Paints." Presented at the IRIS Meeting on Targets, Backgrounds and Discrimination, 12 - 14 February 1985. Proceedings are published by IRIA Center, ERIM, P.O. Box 618, Ann Arbor, MI 48107.

4. G. Bishop and D. M. Weimer, "Fast Phong Shading," Computer Graphics (SIGGRAPH '86 Proceedings), Pages 103-106, August, 1986.

5. M. Segal, C. Korobkin, R. van Widenfelt, J. Foran, and P. Haeberli, "Fast Shadows and Lighting Effects Using Texture Mapping," Proceedings of SIGGRAPH 1993, Pages 249-252, June 1993

6. J. Walker, M. Malkmus, and C.B. Ludwig, "Handbook of the Standardized Infrared Radiation Model (SIRRM) - Vol. I: Technical Manual," Air Force Rocket Propulsion Laboratory Rpt. No. AFRPL-TR-81-61 (August 1981).

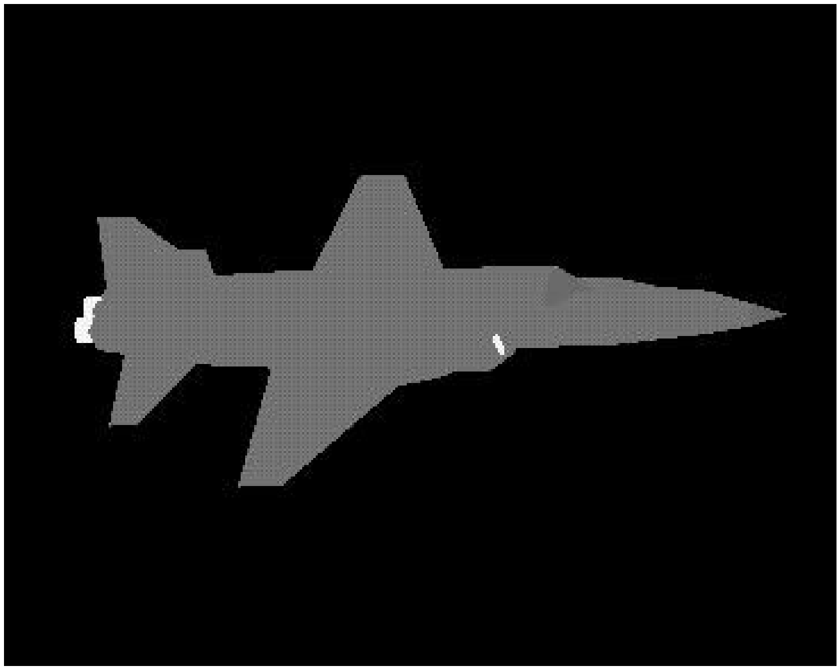

Figure 5 (A). Aircraft thermal emission image for bandpass of 8 to 12 μm.

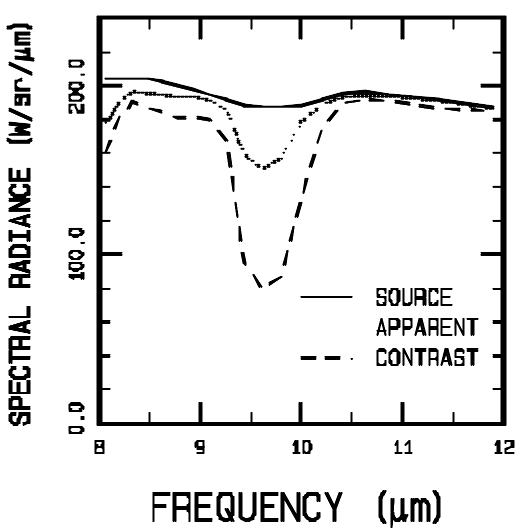

Figure 5 B. Spectral radiance components for image shown in Figure (5)A

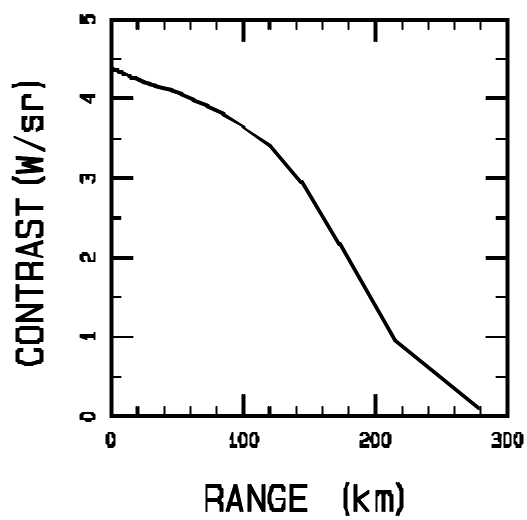

Figure 5 C. Contrast radiance as a function of range for target orientation shown in Figure (5)A

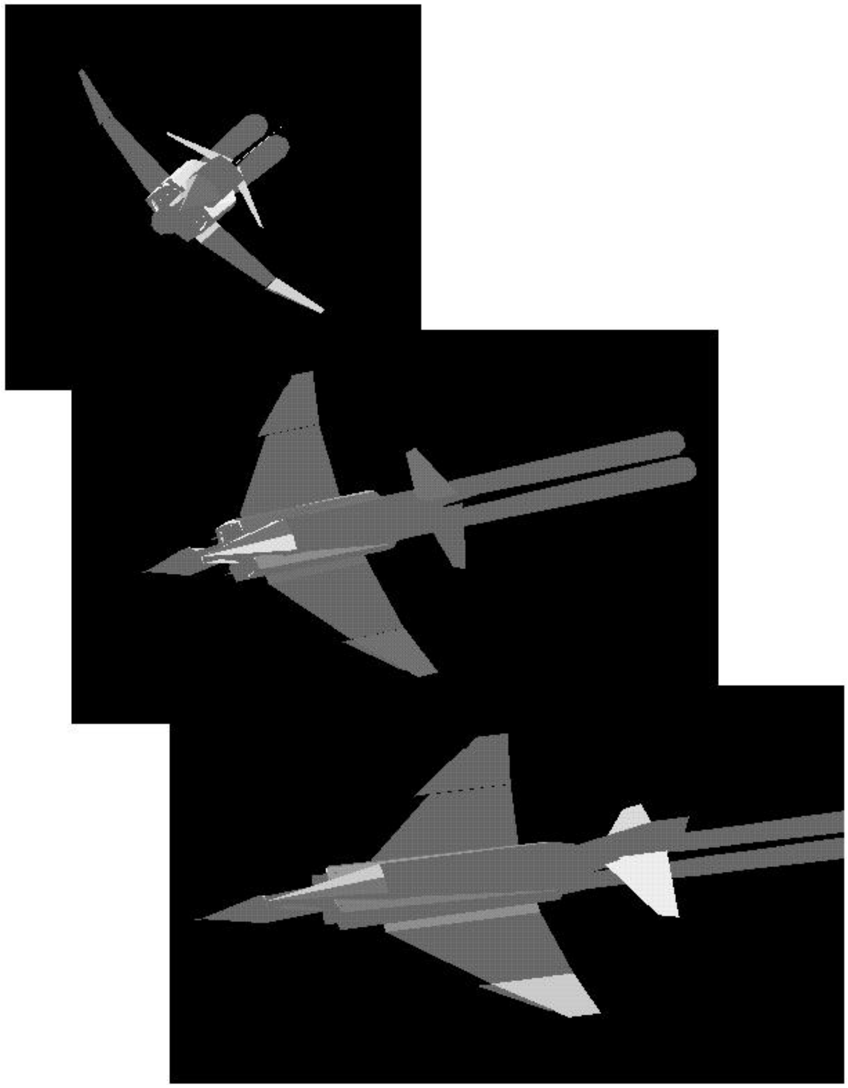

Figure 6. Aircraft radiance images for changing observer aspect angle and a bandpass of 4 to 4.5 μm.